CPC(HEP & NP), 2011, **35**(11): 1037–1041 Chinese Physics C Vol. 35, No. 11, Nov., 2011

Experimental study on scintillation efficiency of ZnO:In to proton response

CHEN Liang(陈亮)[1)] OUYANG Xiao-Ping(欧阳晓平) ZHANG Zhong-Bing(张忠兵)
XIA Liang-Bin(夏良斌) LIU Jin-Liang(刘金良) ZHANG Xian-Peng(张显鹏) LIU Lin-Yue(刘林月)

Northwest Institute of Nuclear Technology, P.O. Box 69-9, Xi'an 710024, China

Abstract: Film ZnO:In crystal is a good candidate for a scintillation recoil proton neutron detection system and the response of ZnO:In to protons is a crucial point. The energy response of ZnO:In to mono-energetic protons in the range of 10 keV–8 MeV was measured. The experiment was carried out in current mode, and Au foil scattering was employed, where the forward scattering protons were used for exciting the sample, and the backward scattering protons were used for monitoring the beam intensity. According to the result, the yield of light non-linearly depends on proton energy, and drops significantly when proton energy is low. The scintillation efficiency as a function of proton energy was obtained, which is very useful for researching the scintillation recoil proton neutron detection system.

Key words: ZnO:In, energy response, scintillation efficiency, proton, neutron detection

PACS: 29.40.Mc, 78.60.Hk, 78.70.Ps **DOI:** 10.1088/1674-1137/35/11/011

1 Introduction

Zinc oxide doped with Ga or In was first reported to have an ultrafast sub-nanosecond time response in the 1960s [1]. However, it is rare to see the utilization of ZnO:Ga or ZnO:In in radiation detection, due to the difficulty in growing high quality ZnO crystals. Most of the research and applications were based on powders, ceramics and thin polycrystalline patterns [2–5]. For example, ZnO:Ga powder has been employed in 14 MeV fusion neutron detection [6], and ZnO:Ga coatings were used for associated α scintillation counting on a DT neutron generator [7]. With the development of crystal growth technologies, doped ZnO crystal film products are now commercially available [8, 9]. Although the film product is still incompetent for spectroscopy or imaging due to its extremely low scintillation efficiency, it works well in pulsed radiation diagnoses, such as sub-nanosecond pulsed X-ray monitoring [10]. Moreover, this film product has been used to build a new scintillation recoil proton neutron detection system (SRPNDS) for pulsed neutron detection.

A traditional recoil proton neutron detection system (RPNDS) is composed of a polythene radiator and a Si-PIN detector to capture the recoil protons, such as the PROTEX [11] configured to measure the total neutron yields of inertial confinement fusion devices. This kind of detector is very useful for intense pulsed neutron intensity monitoring, and can be applied to pulsed neutron spectrum measurement in combination with the neutron time of flight method. However, the sensitivity of the traditional RPNDS is relatively low and difficult to adjust. Si-PIN detectors with large areas are usually employed to increase the recoil proton collection efficiency, but the time response of the Si-PIN detector drops when the area increases, and the time response is more than 10 ns for a Si-PIN detector with a diameter of more than 20 mm. In the new SRPNDS, the Si-PIN detector is replaced by a piece of film ZnO:In crystal. By coupling to an ultrafast photomultiplier tube (PMT), the time response of the SRPNDS can achieve sub-nanoseconds, and its sensitivity is conveniently adjustable by changing PMTs with different gains. In addition, the traditional inorganic scintillator is too slow to be used, and the typical fast organic scintillator which is rich in hydrogen and widely used for

Received 18 February 2011

1) E-mail: jeffnew1982@gmail.com

fast neutron detection is inappropriate as well, because low neutron sensitivity is required to avoid scattering neutron interference.

The response of ZnO:In to recoil protons is key to the SRPNDS. To understand scintillation, the yield of light depends on irradiation particle categories and relates non-linearly to the particle energy [12]. Since the nonlinearity of scintillation efficiency cannot be determined theoretically, the energy response of ZnO:In to protons has been measured experimentally. The scintillation response function could be very useful for optimizing the structure of the SRPNDS, and for studying its sensitivity as well as the spectrum response to neutrons.

2 Experiment

The ZnO:In film crystal is a product from Cermet Inc. [8], with a diameter of ϕ25.4 mm and a thickness of 0.3 mm. Although the time response of ZnO:In is very fast, about 0.65 ns to alpha [9], its scintillation efficiency is extremely low. The typical pulse height spectra to the same ^{241}Am alpha source measured is shown in Fig. 1, where the scintillator for reference is a typical plastic scintillator ST401 with a light yield of about 40% of anthracene. It would be difficult to obtain the individual pulse height spectrum for protons with energies below 1 MeV, because of the interference from the electrical noise of the measuring system. Therefore the current mode measurement was adopted. According to the working process of a scintillation detector, the current output of the PMT can be expressed as

$$I = \Phi \cdot s \cdot L(E_{\rm p}) \cdot p \cdot \eta \cdot G \cdot e, \quad (1)$$

where Φ represents the flux of protons arriving at the sample, s is the effective area under irradiation, $L(E_{\rm p})$ is the light yield for each proton with energy $E_{\rm p}$, p is the light collection efficiency, η and G are the parameters representing the quantum efficiency and gain of the PMT, respectively, and e is the charge of electron. Thus the light yield for each proton with energy $E_{\rm p}$ can be expressed as

$$L(E_{\rm p}) = A\frac{I}{\Phi \cdot s} = A\frac{I \cdot t}{\Phi \cdot s \cdot t} = A\frac{Q}{N}, \quad (2)$$

where A is the inverse of the product of p, η, G, and e. Q is the charge output of the PMT, and N is the number of protons irradiated. As Q and N can be measured absolutely, and A is a constant when the arrangement remains unchanged during the experiment, the relative light yield for ZnO:In to protons with different energies can be measured.

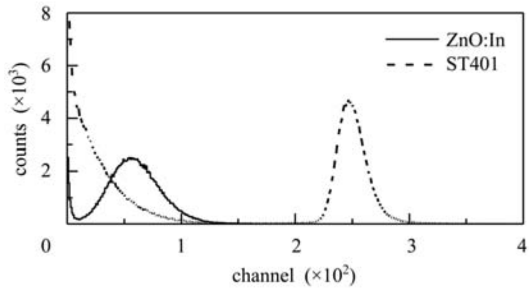

Fig. 1. The pulse height spectrum for ZnO:In and ST401 to ^{241}Am measured under the same condition.

The experiment was carried out on a Van de Graff electrostatic accelerator and a tandem accelerator, respectively, at Peking University, China. As the lowest beam current from the accelerator is about 0.1 nA (about 10^9 particles/s) and it is easy to damage the ZnO:In crystal, the Au foil scattering method was employed to reduce the possibility of damage, where the forward scattering protons are used for exciting the sample, and the backward scattering protons for monitoring. A schematic diagram of the experimental layout is shown in Fig. 2. Beams from two accelerators were guided to the center of a cylindrical vacuum chamber separately from two directions. The Au foil with a thickness of 200 μg/cm^2 was fixed at the center of the chamber and set perpendicular to the beam direction. The ZnO:In crystal was arranged outside the vacuum chamber, 50 cm apart from the target, 30° with respect to both beam directions. The scattering protons have to penetrate a 5 μm (thickness uncertainty <5%) titanium window and 10 mm of air before reaching the ZnO:In crystal. The back of the ZnO:In crystal coupled a PMT, which is a product of the Electron Tubes Limited Company, UK, with a gain of about 10^5 at −1100 V. The current output of the PMT was recorded by an electrometer. The monitor was an Au-Si surface barrier detector, which was set at the back of the Au target inside the vacuum chamber, 165° from the beam direction and 19.5 cm from the target, and the counts of the surface barrier were recorded with a multi-channel analyzer system. The diameters of the collection aperture for the surface barrier detector and the tested sample were ϕ4 mm and ϕ10 mm, respectively.

Since the energy of the protons studied is not very high, the scattering of protons by the Au nucleus is consistent with Rutherford scattering. The ratio of counts between forward and backward testing positions is fixed. For our experimental condition, the ratio of counts between the tested sample and the surface barrier detector is calculated to be about 200.

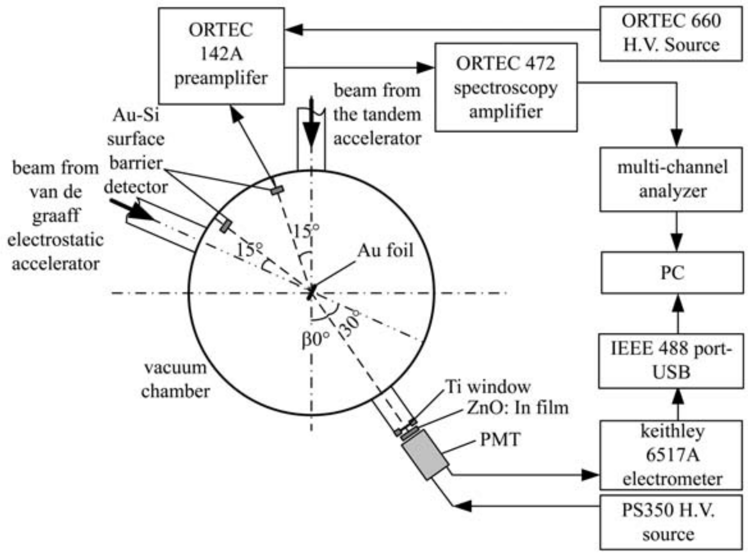

Fig. 2. Experimental setup for the measurement of ZnO:In response to protons using Au-foil scattering.

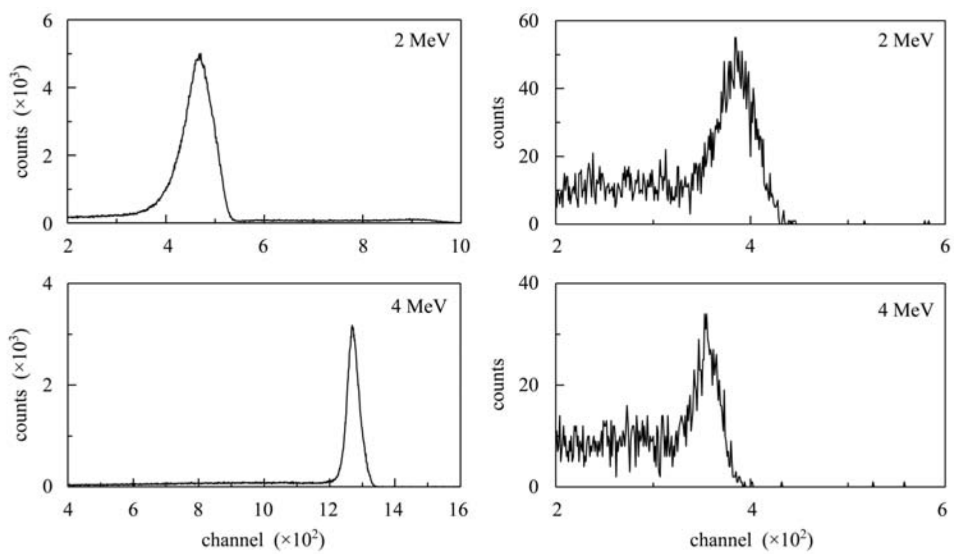

Fig. 3. Scattering proton spectra counted at forward (left) and backward (right) experimental positions simultaneously with Au-Si surface barrier detectors, under the energies of 2 MeV and 4 MeV respectively.

For verification, the ratio was calibrated at the energies of 2 MeV and 4 MeV respectively, by replacing the ZnO:In crystal with another Au-Si surface barrier detector. Both surface barrier detectors were working simultaneously for 5 min, and the spectra were recorded, as shown in Fig. 3. The measured ratio of counts between forward and backward detectors is 197 and 198, respectively at 2 MeV and 4 MeV.

3 Experimental results

Protons with less than 900 keV of energy would be unable to pass through the 5 μm Ti window and 10 mm of air, and protons with energy above 8 MeV would penetrate through the ZnO:In film. The measurement was made for protons with energies in the 900 keV to 8 MeV range, where the Van de Graff electrostatic accelerator generated protons with energy below 2.2 MeV and the tandem accelerator generated protons with energies of above 2.5 MeV. The signals from the PMT and the surface barrier detector were accumulated simultaneously in two minutes, and the results are shown in Table 1. The signal from the PMT was mostly affected by the dark current of the PMT (about 0.1 nA), which had been deducted from the charge recorded, and its contribution to uncertainty was estimated to be 0.006 μC. The pulsed height spectrum recorded from the surface barrier detector suffered from secondary particle interferences, including neutrons, X-rays and gamma rays gene-

Table 1. The experimental results measured under different proton energies.

energy/MeV	energy reaching ZnO:In/MeV	counts of proton[a)]	Q/μC	(Q/N)/pC
0.90	0.012±0.020	107268±5362	0.010±0.006	0.00047±0.00028
0.95	0.050±0.044	70159±3508	0.014±0.006	0.00100±0.00043
1.00	0.165±0.065	35955±1798	0.014±0.006	0.00195±0.00084
1.05	0.275±0.057	37556±1673	0.022±0.006	0.00293±0.00081
1.10	0.372±0.052	50433±2521	0.282±0.006	0.0280±0.0015
1.15	0.463±0.048	17092±854	0.365±0.006	0.1068±0.0056
1.20	0.545±0.046	22175±1108	0.859±0.006	0.1937±0.0098
1.30	0.700±0.043	14472±723	0.984±0.006	0.340±0.017
1.40	0.844±0.041	2710±135	0.258±0.006	0.476±0.026
1.50	0.980±0.040	5325±266	0.588±0.006	0.552±0.028
1.60	1.111±0.037	3860±190	0.518±0.006	0.671±0.034
1.70	1.236±0.036	4282±210	0.641±0.006	0.749±0.037
1.80	1.359±0.036	3044±150	0.572±0.006	0.940±0.047
1.90	1.479±0.035	2621±131	0.571±0.006	1.089±0.056
2.00	1.597±0.035	1770±88	0.425±0.006	1.201±0.062
2.10	1.715±0.034	2954±147	0.739±0.006	1.251±0.063
2.20	1.827±0.035	2327±116	0.633±0.006	1.360±0.069
2.50	2.165±0.035	1865±93	0.685±0.006	1.836±0.093
3.00	2.709±0.034	1311±85	0.612±0.006	2.33±0.15
4.00	3.766±0.033	1005±68	0.662±0.006	3.29±0.23
6.00	5.829±0.032	505±38	0.567±0.006	5.61±0.43
8.00	7.862±0.032	430±35	0.689±0.006	8.01±0.66

[a)] This is the count from the monitoring detector, and N is 200 times the count.

rated from the interaction of protons with their surroundings which caused additional counts distributed over wide channels besides the peak of protons. This interference increased when proton energy was high.

The exact energy of protons reaching the ZnO:In film was simulated using the Geant4 code [13], by modeling according to the experimental configuration. Energy straggling is unavoidable for protons scattered by the Au target, and traversing the Ti window and air, especially for protons with energy of below 1 MeV. The results are also listed in Table 1 (column 2). With the exact proton energy deposited and the ratio of Q/N, the relative light yield for ZnO:In to protons is drawn in Fig. 4, and the results are normalized to the 7.862 MeV data.

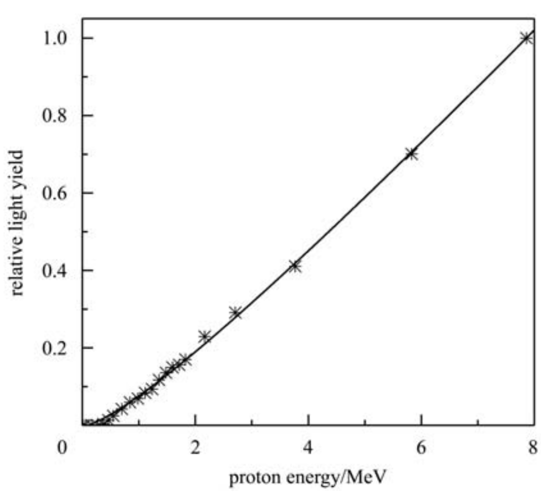

Fig. 4. The normalized light yield of ZnO:In to protons and its fitting with the L. Papadopoulos formula [15], where the quenching parameter of kB is 4.0×10^{-4} cm/MeV.

4 Discussion

According to the dependence of light yield to proton energy in Fig. 4, the yield of light is approximately proportional to the energy deposition when the proton energy is high, but drops significantly for lower energies. This phenomenon is very common among scintillators [12]. Ionization quenching is supposed to be the cause of the decline of scintillation efficiency, and the quenching effect intensifies with ionization density which is directly related to the specific energy loss ($\mathrm{d}E/\mathrm{d}r$). Since the specific energy loss of protons in ZnO increases when the proton energy decreases, the quenching effect becomes obvious for low energy protons. There are many semi-empirical models proposed to describe the radiation luminescence process, considering the processes of the energy deposition, the energy transportation and the luminescence respectively, such as the well known Birks formula [12] as well as the model suggested by K. Michaelian [14] from first principles. L. Papadopoulos [15] introduced a simple and more intelligible model that provides a scintillation response function which resembles the Birks formula:

$$\mathrm{d}L = S\frac{E}{E+kB\lambda\ln(\mu E)}\mathrm{d}E, \quad (3)$$

where S is the absolute scintillation efficiency, kB stands for the quenching parameter. For protons, λ=239.22$\times 10^{-24}N_\mathrm{e}$, and μ=21.785$\times 10^{-4}/\overline{I}$. N_e is the number of electrons per unit volume, and $\overline{I}$ is the mean excitation and ionization potential, which is 1.58$\times 10^{24}$ e/cm^3 and 286 eV respectively for ZnO.

The experimental result was fitted with Eq. (3). Since it was difficult to have a closed-form solution for the integral of Eq. (3), an iterative process was used. For a given kB, the light yield L for each proton energy E could be calculated through numerical integration, and was normalized to the 7.862 MeV result. The result calculated was compared with experimental data, and a loop program was written to find the proper kB minimizing the sum of the square of the difference between experimental data. The final fitting curve is shown in Fig. 4, where kB is 4.0$\times 10^{-4}$ cm/MeV, which is much lower than organic scintillators.

The absolute scintillation efficiency cannot be fitted from experimental results. However, it can be estimated by extending Eq. (3) to α particle irradiation. According to the pulse height spectral shown in Fig. 1, the peak channel for ZnO:In and ST401 is around 56 and 247 respectively, which indicates that the total light yield from ZnO:In is about 0.227 to that of ST401 for α particles with energy of 5.48 MeV. Since the quenching parameter for ST401 is known as 1.29$\times 10^{-2}$ cm/MeV [16], and the parameters of λ and μ in Eq. (3) are determinate for a given irradiation particle and scintillator [15], the ratio of absolute scintillation efficiency between ZnO:In and ST401 is obtained from Eq. (3), which is about 5.9%. As the light yield of ST401 to electrons is about 6400 photons/MeV, the yield of light for ZnO:In is only 380 photons/MeV.

5 Conclusion

The energy response of ZnO:In film crystals to protons ranging from 10 keV to 8 MeV was measured. According to the results, the light yield of ZnO:In depends non-linearly on the proton energy, and drops significantly when the proton energy is low. The scintillation efficiency of ZnO:In as a function of proton energy is obtained, and the quenching parameter for ZnO:In to protons is 4.0$\times 10^{-4}$ cm/MeV. The result would be very useful for research into the scintillation recoil proton neutron detection system.

The authors would like to express their thanks to Professor Wang Jian-yong and Ren Xiao-tang from the Institute of Heavy Ion Physics and the State Key Laboratory of Nuclear Physics and Technology of Peking University, for the experimental conditions provided.

References

1 Luckey D. Nucl. Instrum. Methods, 1968, **62**: 119
2 Tanaka M et al. Appl. Phys. Lett., 2007, **91**: 231117
3 Neal J S, Boatner L A, Giles N C et al. Nucl. Instrum. Methods A, 2006, **568**: 803
4 Bourret-Courchesne E D, Derenzo S E, Weber M J. Nucl. Instrum. Methods A, 2009, **601**: 358
5 WANG Q P, SUN Z, DU J et al. Opt. Mater., 2007, **29**: 1358
6 Chrien R E, Strachan J D. Rev. Sci. Instrum., 1980, **51**: 1638
7 Simpson P J, Tjossem R, Hunt A W et al. Nucl. Instrum. Methods A, 2003, **505**: 82
8 Cermet Inc. http://www.cermetinc.com/
9 Cooper J C, Koltick D S, Mihalczo J T et al. Nucl. Instrum. Methods A, 2003, **505**: 498
10 MA Yan-liang, OU YANG Xiao-ping, CHEN Liang et al. High Power Laser and Particle Beams, 2008, **20**(12): 2088 (in Chinese)
11 Moran M J, Glebov V Y, Stoeckl C et al. Rev. Sci. Instrum., 2005, **76**: 23506
12 Birks J B. The Theory and Practice of Scintillation Counting. Oxford, London, Edinburgh, New York, Paris, Frankfurt: Pergamon Press. 1964. 187
13 Agostinelli S, Allison J, Amako K et al. Nucl. Instrum. Methods A, 2003, **506**: 250
14 Michaelian K, Menchaca-Rocha A, Belmont-Moreno E. Nucl. Instrum. Methods A, 1995, **356**: 297
15 Papadopoulos L, Nucl. Instrum. Methods A, 1999, **434**: 337
16 ZHANG Q M, WANG Q S, XIE Z S et al. Nucl. Instrum. Methods A, 2003, **496**: 146